Mechanisms of the Oxidation and Combustion of Normal Paraffin Hydrocarbons: Transition from $C_1–C_{10}$ to $C_{11}–C_{16}$

V. Ya. Basevich, A. A. Belyaev, V. S. Posvyanskii, and S. M. Frolov

Semenov Institute of Chemical Physics, Russian Academy of Sciences, Moscow, Russia
e-mail: basevich@center.chph.ras.ru
Received April 6, 2012

Abstract—Recently, detailed kinetic mechanisms of the oxidation and combustion of higher hydrocarbons, composed of hundreds of components and thousands of elementary reactions, have been proposed. Despite the undoubtful advantages of such detailed mechanisms, their application to simulations of turbulent combustion and gas dynamic phenomena is difficult because of their complexity. At the same time, to some extent limited, they cannot be considered exhaustive. This work applies previously proposed algorithm for constructing an optimal mechanism of the high- and low-temperature oxidation and combustion of normal paraffin hydrocarbons, which takes into account the main processes determining the reaction rate and the formation of key intermediates and final products. The mechanism has the status of a nonempirical detailed mechanism, since all the constituent elementary reactions have a kinetic substantiation. The mechanism has two specific features: (1) it does not include reactions of so-called double oxygen addition (first to the peroxide radical, and then to its isomeric form), i.e., the first addition turns out to be sufficient; (2) it does not include isomeric compounds and their derivatives as intermediates, since this oxidation pathway is slower than the oxidation of molecules and radicals with normal structure. Application of the algorithm makes it possible to compile a compact mechanism, which is important for modeling chemical processes involving paraffin hydrocarbons C_n with large n. Previously, based on this algorithm, compact mechanisms of the oxidation and combustion of propane, *n*-butane, *n*-pentane, *n*-hexane, *n*-heptane, *n*-octane, *n*-nonane, and *n*-decane have been constructed. In this work, we constructed a nonempirical detailed mechanism of the oxidation and combustion of hydrocarbons from *n*-undecane to *n*-hexadecane. The most important feature of the new mechanism is its staged nature, which manifests itself through the emergence of cool and blue flames during low-temperature autoignition. The calculation results are compared with experimental data.

Keywords: autoignition, paraffin hydrocarbons, kinetic mechanisms

DOI: 10.1134/S1990793113020103

INTRODUCTION

Recently, detailed mechanisms of the oxidation and combustion of higher hydrocarbons, containing hundreds of components and thousands of elementary reaction steps, have been proposed. These mechanisms include a variety of intermediate stable molecules and radicals arising during the oxidation and combustion of hydrocarbons. For example, the mechanism for *n*-heptane proposed in [1] includes 650 species and 2300 reactions, whereas in [2], for a number of hydrocarbons from *n*-octane to *n*-hexadecane, a mechanism containing 8130 reactions involving 2116 components was developed. Despite the undeniable advantages of detailed mechanisms, their application to solving multidimensional problems of combustion gas dynamics is difficult because of their complexity. Moreover, consideration of all possible isomers of the components and all the reactions between all the components would make such mechanisms much larger (for example, by inclusion of polycyclic aromatic hydrocarbons, soot, vibra-

tionally exited molecules, reactions of their formation and consumption, etc. [3, 4]).

In addition, the construction of such mechanisms involves a variety of uncertainties associated with the lack of many necessary and reliable data on thermochemistry and reaction rate constants. This affects the validity and accuracy of the kinetic mechanism. Lastly, all available publications on the subject contain no information on the applicability of the proposed detailed kinetic mechanisms to describing a multistep low-temperature oxidation of hydrocarbons [5, 6], accompanied by the occurrence of not only cool but also blue flames [7].

Thus, the known detailed kinetic mechanisms are generally incomprehensive and, to a certain degree, limited. At the same time, for specific problem in which the main processes that determine the reaction rate and the formation of key intermediates and final products should be considered, optimal rather than maximal mechanisms of oxidation and combustion of hydrocarbons are of interest. Such mechanisms, even

compact, do not lose the status of nonempirical detailed mechanisms as long as all the constituent elementary reactions have a kinetic substantiation. In other words, in simulating the oxidation and combustion of hydrocarbons, there always exists the possibility of a nonextensive construction of mechanisms with a desired limitation of the diversity of products and reactions, but retaining the main channels of the process and fundamentally important types of elementary steps.

The reactions of paraffinic hydrocarbons are known to have many common phenomenological features [5−8]. This commonality enables to apply the algorithm previously used for developing the chemical mechanism of the oxidation and combustion of paraffin hydrocarbons from propane to n-decane [8−13] to constructing a mechanism of the oxidation and combustion of the following members of the homologous series, from n-undecane (n-$C_{11}H_{24}$) to n-hexadecane (n-$C_{16}H_{34}$). This algorithm is based on the principle of a nonextensive construction of the mechanism proceeding from two assumptions: (1) low-temperature branching is described by a group of reactions with a single addition of oxygen, and (2) the channels of oxidation via isomeric forms can be excluded from consideration because they are slower than the oxidation through nonisomerized components.

Regarding the first assumption, it is worthwhile to note that the cool-flame kinetics of the oxidation of hydrocarbons is sometimes described within the framework of schemes with so-called double oxygen addition: first to a peroxide radical and then to its isomerized form [4]. Since the available databases contain no experimental data on the reaction rates required to describe the process of double addition, the authors of works in which double addition is nevertheless considered use only speculative estimates. However, the need for the second addition of oxygen in the quantitative interpretation of reaction rates has not yet been proven: in the oxidation of CH_4 and C_2H_6, such reactions are hindered because of a structural stress, whereas for heavier hydrocarbons, such as propane [8] and even n-decane [13], a satisfactory description of the available experimental data was performed considering only the first addition. This is consistent with the known fact that, in chemical kinetics under given thermochemical conditions, two reactions are very rarely able to make equivalent contributions to the process of oxidation. Therefore, in [8−13], it was assumed that the low-temperature branching for alkanes from C_3H_8 to n-decane is described by a group of reactions with addition of one oxygen. This group includes reactions that provide low-temperature oxidation:

$$R + O_2 = RO_2,$$

$$RO_2 + RH = RO_2H + R,$$

$$RO_2H = RO + OH,$$
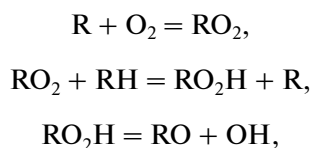
(RH is the initial hydrocarbon and R is the hydrocarbon radical), which are followed by other reactions of decomposition and oxidation of radicals and molecules.

Note that the mechanisms of the oxidation of C_nH_{2n+2} at $n > 10$ have been proposed previously (see, e.g., [2−4]), but none of these mechanisms was demonstrated to adequately describe the multistage oxidation of hydrocarbons accompanied not only by cool but also by blue flames in the course of autoignition. Therefore, the development of mechanisms of the oxidation and combustion of paraffin hydrocarbons up to $n = 16$ on the basis of the nonextensive approach is important and useful in practice, since such heavy hydrocarbons are present in motor fuels.

CONSTRUCTION OF THE MECHANISM

According to the algorithm from [8−13], the kinetic mechanism of the oxidation of C_nH_{2n+2} hydrocarbons is based on the mechanism for the preceding member of the homologous series of carbon atoms, $C_{(n−1)}H_{2(n−1)+2}$. This applies to both the reactants and reactions. For example, for n-undecane, the preceding analogue in the homologous series is n-decane; therefore, the mechanism for n-undecane was based on the mechanism of the oxidation and combustion of the $C_1−C_{10}$ hydrocarbons, comprising 108 components and 1083 reactions [13]. The algorithm from [8−13] was implemented as a computer code which selects new components, new reactions, and their Arrhenius parameters. The table lists new components for each n of $n = 11, ..., 16$.
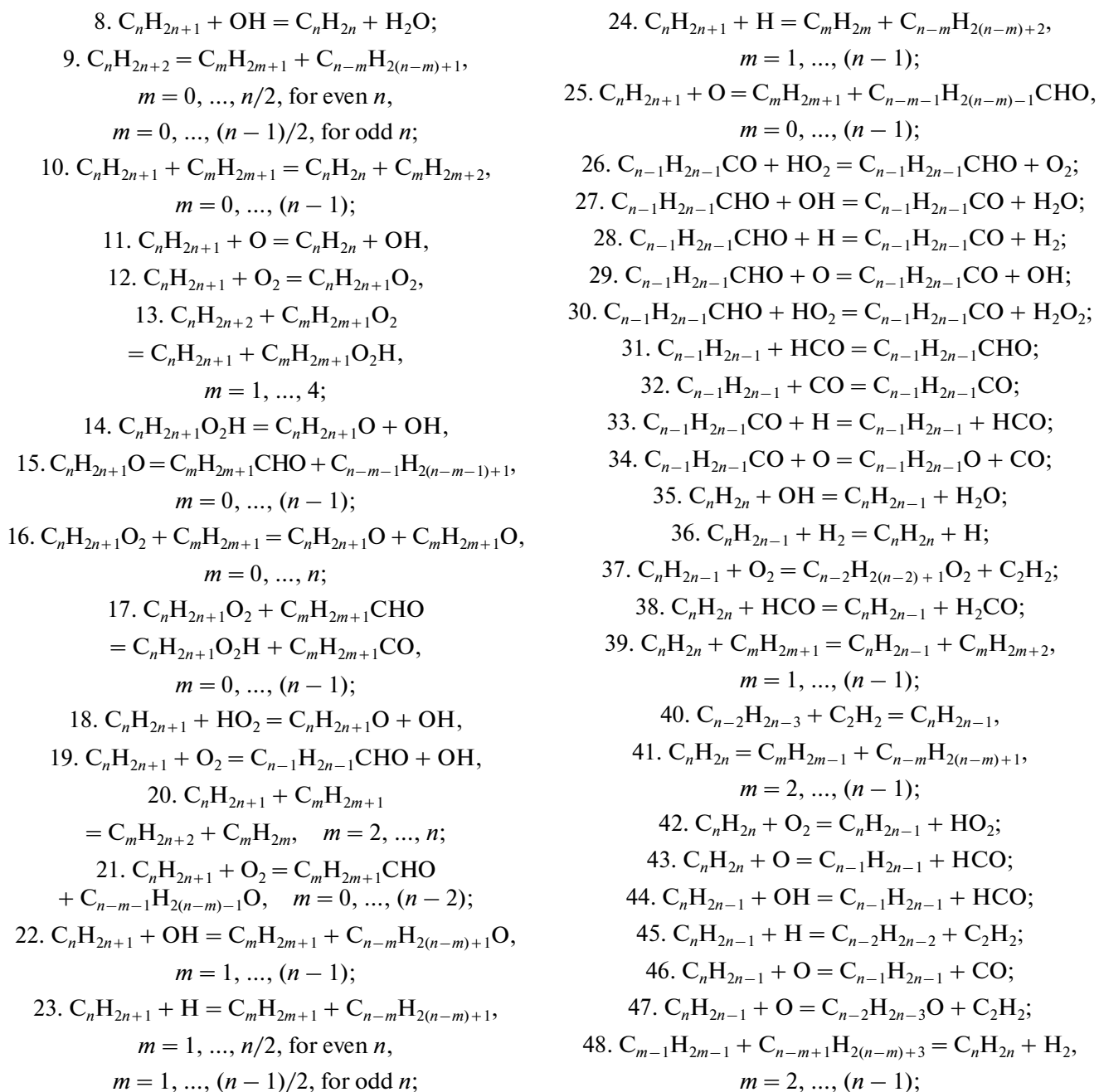
Using the recommendations from [14], we calculated the enthalpy of formation ΔH°_{f298}, the entropy S°_{298}, and the coefficients of the polynomial for the isobaric heat capacity, $c_p = c_0 + c_1 T/10^3 + c_2 T^2/10^6 + c_3 T^3/10^9$, for the selected components by applying the rules of additivity. For each addition of a CH_2 group to the components of the mechanism of the oxidation of n-decane, the enthalpy and entropy of formation were changed by −4.932 kcal/mol and 9.564 cal mol^{-1} K^{-1}, respectively, whereas the coefficients of the polynomial for the isobaric heat capacity, c_0, c_1, c_2, and c_3 (dimension of c_p, cal mol^{-1} K^{-1}), by 0.3934, 0.021363, −0.1197 · 10^{-4}, and 0.2596 · 10^{-8}, respectively.

Below are given the new reactions for each $n = 11, ..., 16$:

1. $C_nH_{2n+2} + O_2 = C_nH_{2n+1} + HO_2$;
2. $C_nH_{2n+2} + OH = C_nH_{2n+1} + H_2O$;
3. $C_nH_{2n+2} + H = C_nH_{2n+1} + H_2$;
4. $C_nH_{2n+2} + O = C_nH_{2n+1} + OH$;
5. $C_nH_{2n+2} + HO_2 = C_nH_{2n+1} + H_2O_2$;
6. $C_nH_{2n} + H = C_nH_{2n+1}$;
7. $C_nH_{2n+1} + O_2 = C_nH_{2n} + HO_2$;

Reactants of the mechanism of oxidation and combustion of *n*-hydrocarbons

No.	Component	Formula
1	Normal paraffin hydrocarbon	C_nH_{2n+2}
2	Hydrocarbon radical	C_nH_{2n+1}
3	Peroxy radical	$C_nH_{2n+1}O_2$
4	Hydroperoxide	$C_nH_{2n+1}O_2H$
5	Oxyradical	$C_nH_{2n+1}O$
6	Aldehyde	$C_{n-1}H_{2(n+1)+1}CHO$
7	Aldehyde radical	$C_{n-1}H_{2(n+1)+1}CO$
8	Unsaturated hydrocarbon	C_nH_{2n}
9	Unsaturated hydrocarbon radical	C_nH_{2n-1}

8. $C_nH_{2n+1} + OH = C_nH_{2n} + H_2O;$

9. $C_nH_{2n+2} = C_mH_{2m+1} + C_{n-m}H_{2(n-m)+1},$
$m = 0, ..., n/2,$ for even $n,$
$m = 0, ..., (n-1)/2,$ for odd $n;$

10. $C_nH_{2n+1} + C_mH_{2m+1} = C_nH_{2n} + C_mH_{2m+2},$
$m = 0, ..., (n-1);$

11. $C_nH_{2n+1} + O = C_nH_{2n} + OH,$

12. $C_nH_{2n+1} + O_2 = C_nH_{2n+1}O_2,$

13. $C_nH_{2n+2} + C_mH_{2m+1}O_2$
$= C_nH_{2n+1} + C_mH_{2m+1}O_2H,$
$m = 1, ..., 4;$

14. $C_nH_{2n+1}O_2H = C_nH_{2n+1}O + OH,$

15. $C_nH_{2n+1}O = C_mH_{2m+1}CHO + C_{n-m-1}H_{2(n-m-1)+1},$
$m = 0, ..., (n-1);$

16. $C_nH_{2n+1}O_2 + C_mH_{2m+1} = C_nH_{2n+1}O + C_mH_{2m+1}O,$
$m = 0, ..., n;$

17. $C_nH_{2n+1}O_2 + C_mH_{2m+1}CHO$
$= C_nH_{2n+1}O_2H + C_mH_{2m+1}CO,$
$m = 0, ..., (n-1);$

18. $C_nH_{2n+1} + HO_2 = C_nH_{2n+1}O + OH,$

19. $C_nH_{2n+1} + O_2 = C_{n-1}H_{2n-1}CHO + OH,$

20. $C_nH_{2n+1} + C_mH_{2m+1}$
$= C_mH_{2n+2} + C_mH_{2m}, \quad m = 2, ..., n;$

21. $C_nH_{2n+1} + O_2 = C_mH_{2m+1}CHO$
$+ C_{n-m-1}H_{2(n-m)-1}O, \quad m = 0, ..., (n-2);$

22. $C_nH_{2n+1} + OH = C_mH_{2m+1} + C_{n-m}H_{2(n-m)+1}O,$
$m = 1, ..., (n-1);$

23. $C_nH_{2n+1} + H = C_mH_{2m+1} + C_{n-m}H_{2(n-m)+1},$
$m = 1, ..., n/2,$ for even $n,$
$m = 1, ..., (n-1)/2,$ for odd $n;$

24. $C_nH_{2n+1} + H = C_mH_{2m} + C_{n-m}H_{2(n-m)+2},$
$m = 1, ..., (n-1);$

25. $C_nH_{2n+1} + O = C_mH_{2m+1} + C_{n-m-1}H_{2(n-m)-1}CHO,$
$m = 0, ..., (n-1);$

26. $C_{n-1}H_{2n-1}CO + HO_2 = C_{n-1}H_{2n-1}CHO + O_2;$

27. $C_{n-1}H_{2n-1}CHO + OH = C_{n-1}H_{2n-1}CO + H_2O;$

28. $C_{n-1}H_{2n-1}CHO + H = C_{n-1}H_{2n-1}CO + H_2;$

29. $C_{n-1}H_{2n-1}CHO + O = C_{n-1}H_{2n-1}CO + OH;$

30. $C_{n-1}H_{2n-1}CHO + HO_2 = C_{n-1}H_{2n-1}CO + H_2O_2;$

31. $C_{n-1}H_{2n-1} + HCO = C_{n-1}H_{2n-1}CHO;$

32. $C_{n-1}H_{2n-1} + CO = C_{n-1}H_{2n-1}CO;$

33. $C_{n-1}H_{2n-1}CO + H = C_{n-1}H_{2n-1} + HCO;$

34. $C_{n-1}H_{2n-1}CO + O = C_{n-1}H_{2n-1}O + CO;$

35. $C_nH_{2n} + OH = C_nH_{2n-1} + H_2O;$

36. $C_nH_{2n-1} + H_2 = C_nH_{2n} + H;$

37. $C_nH_{2n-1} + O_2 = C_{n-2}H_{2(n-2)+1}O_2 + C_2H_2;$

38. $C_nH_{2n} + HCO = C_nH_{2n-1} + H_2CO;$

39. $C_nH_{2n} + C_mH_{2m+1} = C_nH_{2n-1} + C_mH_{2m+2},$
$m = 1, ..., (n-1);$

40. $C_{n-2}H_{2n-3} + C_2H_2 = C_nH_{2n-1},$

41. $C_nH_{2n} = C_mH_{2m-1} + C_{n-m}H_{2(n-m)+1},$
$m = 2, ..., (n-1);$

42. $C_nH_{2n} + O_2 = C_nH_{2n-1} + HO_2;$

43. $C_nH_{2n} + O = C_{n-1}H_{2n-1} + HCO;$

44. $C_nH_{2n-1} + OH = C_{n-1}H_{2n-1} + HCO;$

45. $C_nH_{2n-1} + H = C_{n-2}H_{2n-2} + C_2H_2;$

46. $C_nH_{2n-1} + O = C_{n-1}H_{2n-1} + CO;$

47. $C_nH_{2n-1} + O = C_{n-2}H_{2n-3}O + C_2H_2;$

48. $C_{m-1}H_{2m-1} + C_{n-m+1}H_{2(n-m)+3} = C_nH_{2n} + H_2,$
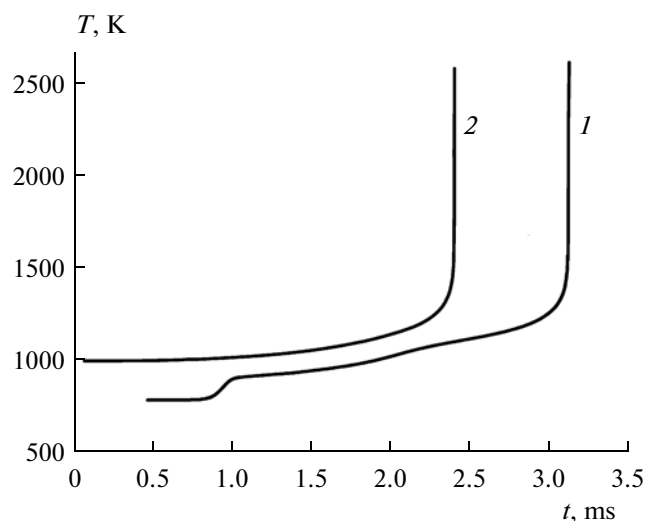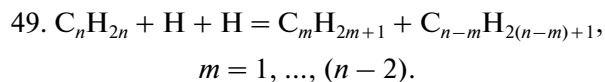$m = 2, ..., (n-1);$

Fig. 1. Calculated time histories of the gas temperature for the autoignition of a *n*-hexadecane–air stoichiometric mixture at $P_0 = 15$ atm and $T_0 = $ (*1*) 787 K and (*2*) 1000 K.

49. $C_nH_{2n} + H + H = C_mH_{2m+1} + C_{n-m}H_{2(n-m)+1}$,

$$m = 1, ..., (n - 2).$$

Here, the expression $m = 0, ..., n$ means that m is varied from 0 to n, where n is number of carbon atoms in a particular chemical component. The mechanisms for *n*-undecane was extended compared to the mechanism for *n*-decane to include nine new components and 180 elementary steps, so that the mechanism for *n*-undecane was comprised of 117 components and 1263 reactions. The respective figures for the rest of the studied alkanes are: *n*-dodecane, 126 components and 1459 reactions; *n*-tridecane, 135 components and 1667 reactions; *n*-tetradecane, 144 components and 1892 reactions; *n*-pentadecane, 153 components, and 2128 reactions; and *n*-hexadecane, 162 components and 2380 reactions (each reaction is taken into account in both forward and reverse).

When evaluating the kinetic parameters of the new reactions, we assumed, as in [8–13], that the rate constants for the mechanism of propane oxidation [8] are quite satisfactory and can be used to compile arrays of rate constants for more complex hydrocarbons on the basis of the expressions for the two-parameter form of the rate constant for the *i*th reaction with preexponential factor A_i and activation energy E_i:

$$A_{i(n)} = A_{i(n=3)} \exp[(\Delta S_{i(n)} - \Delta S_{i(n=3)})/R], \quad (1)$$

$$E_{i(n)} = E_{i(n=3)} - 0.25(\Delta H_{i(n)} - \Delta H_{i(n=3)}) \quad (2)$$

for exothermic reactions and

$$E_{i(n)} = E_{i(n=3)} + 0.75(\Delta H_{i(n)} - \Delta H_{i(n=3)}) \quad (3)$$

for endothermic reactions, where R is the universal gas constant, $\Delta S_{i(n)}$ and $\Delta S_{i(n=3)}$ are the respective entropy changes and $\Delta H_{i(n)}$ and $\Delta H_{i(n=3)}$ are the respective enthalpy changes of the reactions.

The emergence of cool and blue flames during multistage autoignition is a graphic manifestation of critical phenomena in chemical kinetics. It is known that critical phenomena are multifunctional and appear at a certain ratio of the rates of different elementary events. Therefore, the kinetic modeling of such phenomena requires additional analysis and selection of the rate constants of the most important reactions within a theoretically acceptable range not exceeding the experimental error. In other words, a simple substitution of approximate values of the key rate constants not always provides a description of the observed critical phenomena. For the constructed mechanisms of the oxidation of paraffin hydrocarbons with $n = 11, ..., 16$, such an adjustment of the rate constants was required for a limited number of reactions, namely the reactions of these hydrocarbons with hydroperoxide radicals and of alkyl radicals with molecular oxygen.

VERIFICATION OF THE MECHANISM

Autoignition of Gas Mixtures

The predictive ability of the mechanism was tested by comparing the calculation results with the available experimental data on the autoignition of the studied hydrocarbons. Given that direct measurements for these hydrocarbons are scarce, it is necessary to use indirect data to test the mechanisms. The calculations were performed using the standard kinetic code previously used in [8–13].

Figure 1 shows typical calculated time dependences of the temperature for the autoignition of a stoichiometric air–*n*-hexadecane mixture at relatively low (787 K) and high (1000 K) initial temperatures. As can be seen, at the high initial temperature, the autoignition occurs as a single-stage process: the temperature increases monotonically without any specific features in the $T(t)$ curve, with the mixture exploding at $t \approx 2.4$ ms. At the low initial temperature, the autoignition behaves as a multistage process, with the sequential appearances of cool and blue flames, followed by a hot explosion. The first stepwise rise in the $T(t)$ curve, associated with the occurrence of a cool flame, occurs at $t \approx 0.9$ ms. Later, at $t \approx 2$ ms, a blue flame appears, followed, at $t \approx 3.2$ ms, by a hot explosion, raising the temperature to above 2500 K.

The acceleration of the reaction over the cool-flame period is a result of the branching associated with the decomposition of alkyl hydroperoxide ($C_{16}H_{33}O_2H$ here) to the hydroxyl and oxyradical. A blue flame arises due to the branching caused by the decomposition of hydrogen peroxide H_2O_2. This conclusion is supported by the behavior of the calculated kinetic curves for the peroxides and two peaks in the curve for the hydroxyl concentration (Fig. 2). The hot explosion occurs due to the branched-chain reaction of atomic hydrogen H with molecular oxygen O_2. Note
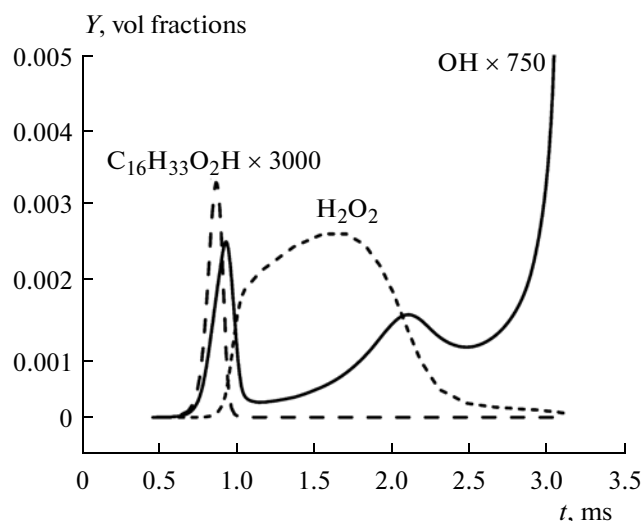
Fig. 2. Calculated time histories of the dimensionless concentrations of peroxides and hydroxyl for the autoignition of a n-hexadecane–air stoichiometric mixture at $T_0 = 787$ K and $P_0 = 15$ atm.
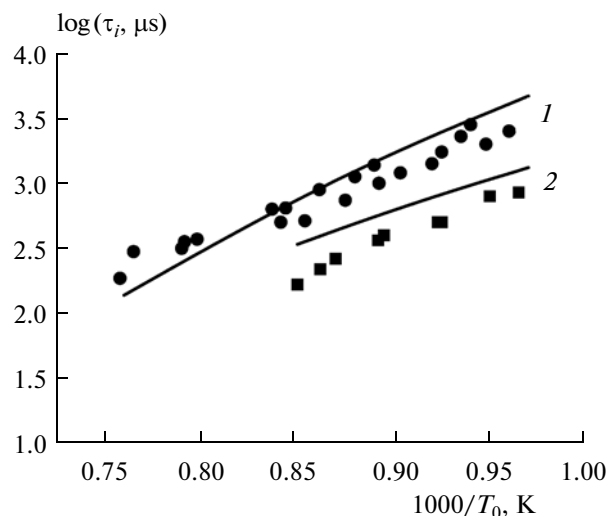

Fig. 3. Comparison of the calculated (curves) and measured (symbols [15, 16]) dependences of the ignition delay times τ_i on the initial temperature T_0 for a $0.0562C_{12}H_{26}$–$0.21O_2$–Ar mixture at $P_0 = (1, \bullet)$ 6.7 and $(2, \blacksquare)$ 20 atm.

that, in experiments, such a pronounced separation of the stages may not be detected due to temperature inhomogeneities; however, in reality, it should manifest itself locally.

The developed kinetic mechanism was compared with the available experimental data for the ignition of $C_{12}H_{26}$. Figure 3 shows the calculated (curves) and measured (symbols [15, 16]) temperature dependences of the ignition delay times for a $0.00562C_{12}H_{26}$–$0.21O_2$–Ar mixture (with an equivalence ratio of $\Phi = 0.5$) at initial pressures of $P_0 = 6.7$ and 20.0 atm. Based on the data from [17, 18], we plotted the experimental pressure dependence of the ignition delay time for a n-dodecane–air mixture ($\Phi = 0.5$) and compared it with the theoretical curve (Fig. 4). The papers [17, 18] also report the experimental temperature dependence of the ignition delay time for the same mixture over a wide temperature range, including the region of negative temperature coefficient (NTC) at the pressure of 20 atm. A comparison of the calculation results with these experimental data is shown in Fig. 5. Figure 6 compares our calculation results with the experimental data from [19] on the time evolution of the concentrations of the components behind a shock wave in a n-dodecane–air–argon mixture. Figure 7 compares the calculated ignition delay time with the experimental data from [17] for n-tetradecane ($C_{14}H_{30}$)–air mixtures of different compositions.

Figure 8 shows the calculated dependence of the ignition delay times for stoichiometric mixtures of air with hydrocarbons with $n = 3$–7, 10 and 16 on the initial temperature at a fixed initial pressure, $P_0 = 15$ atm. As can be seen, the behavior of the dependences is qualitatively the same for all these hydrocarbons. Ear-

lier [8–13], the calculation results for $n = 3$–7, 10 were compared with experimental data, so the consistency of the results observed for $n = 3$, 7, 10 and for $n = 16$ can be considered as indirect evidence of a satisfactory simulation of the ignition delay time for hydrocarbons with $n = 11, ..., 16$. The most important feature of all these hydrocarbon–air mixtures is the manifestation of a multistage autoignition: at low and medium temperatures, all the curves exhibit a region with a negative or zero temperature coefficient of the reaction rate, when the total ignition delay time at high initial temperatures is longer than at low temperatures.

Figure 9 shows the ignition delay for stoichiometric mixtures of air with paraffin hydrocarbons with $n = 3$–16 at the initial temperature of $T_0 = 787$ K and the initial pressure of $P_0 = 15$ atm. Here, the closed symbols were obtained by processing the published experimental data, the closed square is the result of extrapolation using an exponential function, whereas the curve represents the results of calculations within the framework of the detailed mechanism of the oxidation of n-hexadecane in which all the hydrocarbons up to $n = 16$ were taken into account.

Laminar Flame Propagation

To test the developed kinetic mechanism, we additionally calculated the laminar flame speed u_n for n-dodecane–air mixtures with different fuel-to-air equivalence ratios Φ at atmospheric pressure and initial temperatures of $T_0 = 400$ and 470 K, using a one-dimensional computer code [20]. Figure 10 compares the calculated values with the experimental data [21].
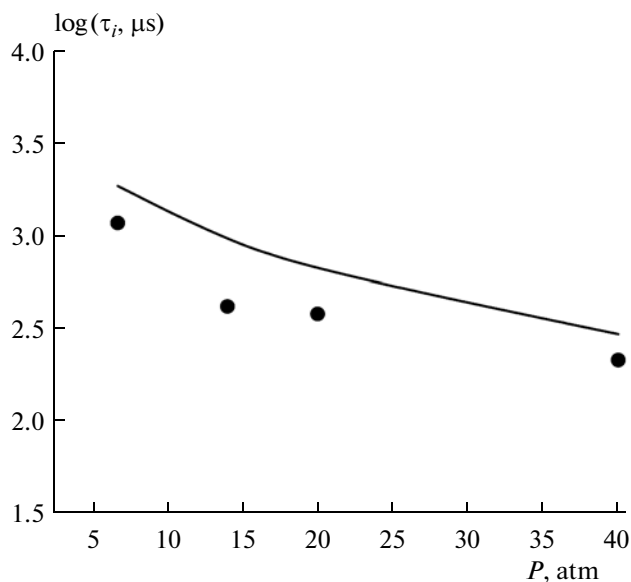
Fig. 4. Comparison of the calculated (curves) and measured (symbols [17, 18]) dependences of the ignition delay times τ_i on the pressure for a n-dodecane–air mixture with $\Phi = 0.5$ at $T_0 = 1100$ K.
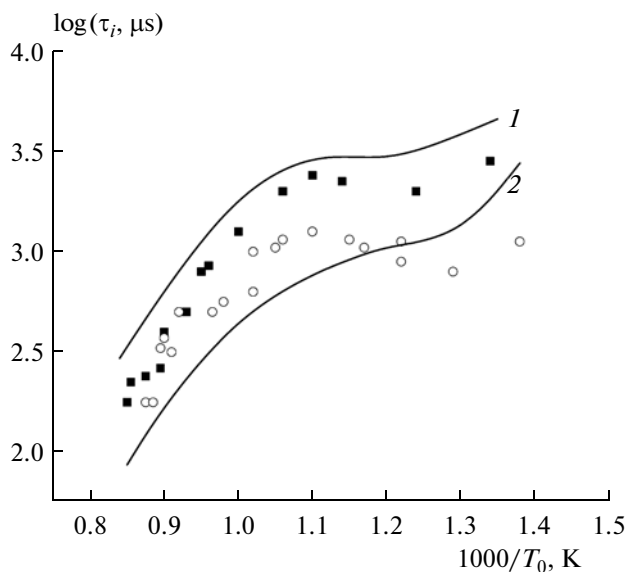
Fig. 5. Comparison of the calculated (curves) and measured (symbols [17, 18]) dependences of the ignition delay times τ_i on the initial temperature for n-dodecane–air mixtures with $\Phi = (1, \blacksquare)$ 0.5 and $(2, \circ)$ 1.0 at $P_0 = 20$ atm.
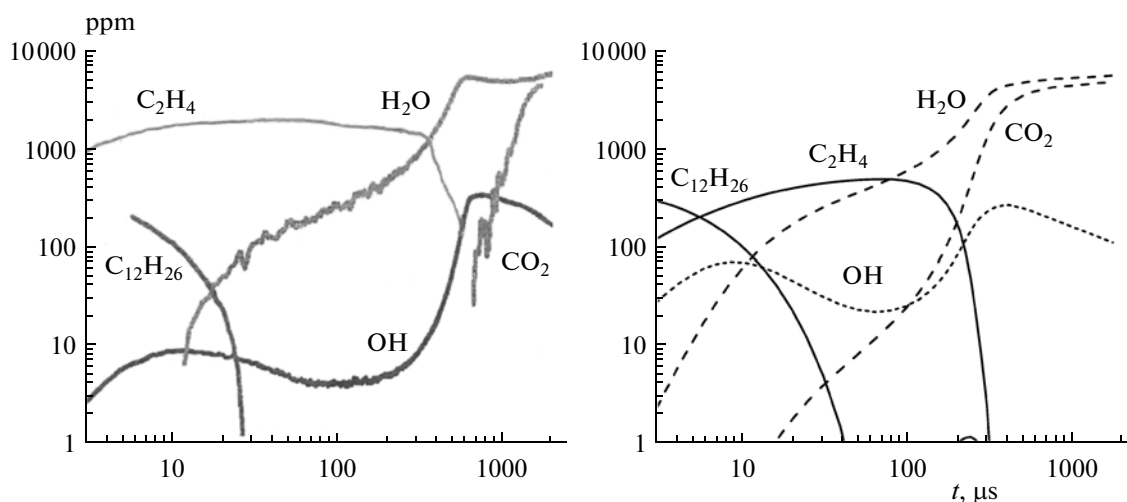

Fig. 6. Comparison of the experimental [19] (left) with calculated (right) time profiles of the concentrations of the components behind a shock wave in a 457 ppm n-dodecane–O_2–Ar mixture at $\Phi = 1.0$, $T_0 = 1410$ K, and $P_0 = 2.3$ atm.

Autoignition of Fuel Droplets

The developed detailed kinetic mechanisms were also applied to calculating the characteristics of the ignition and combustion of droplets of the studied individual hydrocarbons. The calculations were performed using the time-dependent one-dimensional (spherical symmetry) equations of conservation of mass, chemical species, and energy for the gas and condensed phases with matching of the solutions at the droplet surface. A detailed description of the mathematical model and calculation method is given in [22]. The initial temperature T_{g0} of the air around the droplet was varied, whereas the initial temperature

of the liquid was always 293 K. The initial radius of the computational domain R_0 around the droplet was much more than the initial radius of the droplet r_0. According to [22], to any chosen value of R_0 corresponds a specific value of the fuel-to-oxidizer equivalence ratio Φ in a uniform monodisperse droplet mixture. After an induction period, at a certain distance from the center of the droplet, gas autoignited.

Solution of the problem for single droplets of different sizes and for uniform monodisperse droplet mixtures over a wide range of pressures, initial air temperatures, and initial mixture compositions Φ revealed the same multistage nature of the process of oxidation as in
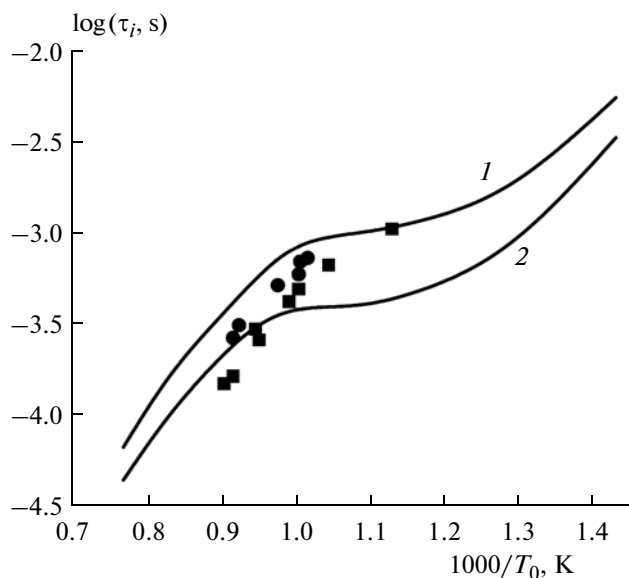
Fig. 7. Comparison of the calculated (curves) and measured (symbols [17]) dependences of the ignition delay times τ_i on the initial temperature for n-tetradecane−air mixtures with $\Phi = (1, \bullet)$ 0.5 and $(2, \blacksquare)$ 1.0 at $P_0 = 40$ atm.
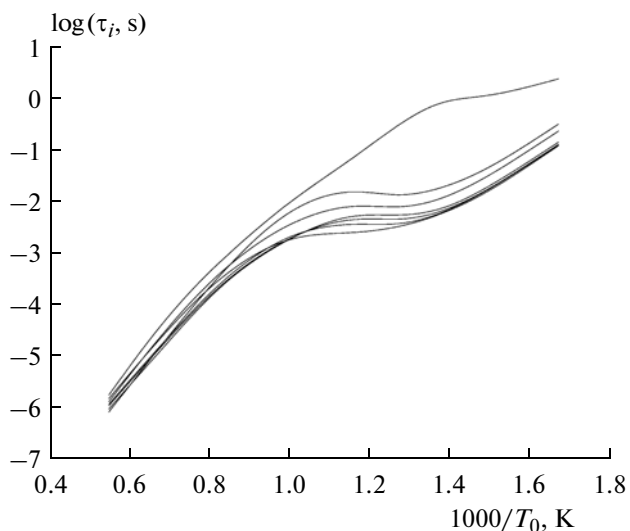

Fig. 8. Comparison of the calculated dependences of the ignition delay times τ_i on the initial temperature for stoichiometric mixtures of air with various hydrocarbons ($n = 3-7$, 10, 16 for curves from top to bottom) at $P_0 = 15$ atm.
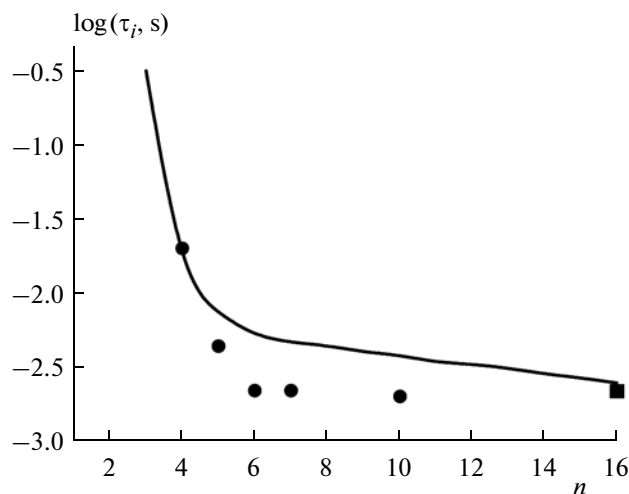
Fig. 9. Comparison of the calculated (curve) and measured (symbols) ignition delay times τ_i for stoichiometric mixtures of paraffin hydrocarbons C_nH_{2n+2} with various n at $T_0 = 787$ K and $P_0 = 15$ atm: ($\bullet$) results of processing experimental data and ($\blacksquare$) extrapolation result.
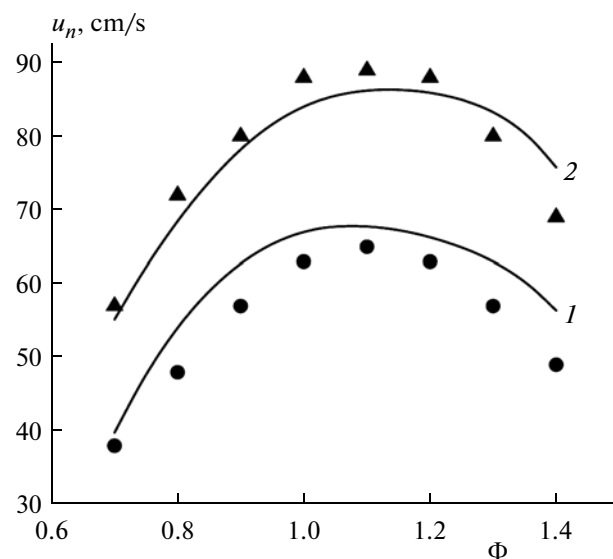
Fig. 10. Comparison of the calculated (curve) measured (symbols [21]) dependences of the laminar flame speed u_n on the fuel-to-oxidizer equivalence ratio Φ for a n-dodecane−air mixture at $P_0 = 1$ atm and $T_0 = (1, \bullet)$ 400 and $(2, \blacktriangle)$ 470 K.

the autoignition of gas mixtures. Figure 11 shows the calculated time histories of the maximum gas temperature for the autoignition of n-tetradecane drops at an initial pressure of $P_0 = 20$ atm and various initial air temperatures: $T_{g0} = 750$, 850, 1000, and 1200 K. The calculations were performed for droplets with $d_0 = 2r_0 = 60$ μm and a fuel-to-oxidizer equivalence ratio of $\Phi = 1$, calculated from the masses of the liquid fuel and air (initial concentration of fuel vapor in the air was zero).

As can be seen, the curves in Fig. 11 are very similar to those in Fig. 1; i.e., for the autoignition of droplets, the curves of maximum temperature of the gas phase feature successive cool and blue flames followed by a hot explosion. Note that cool flames were observed experimentally during the autoignition of a spray [23].

Figure 12 shows the calculated temperature dependence of the maximum temperature $T_{g, max}$ of the gas around the droplets and the square of the droplet
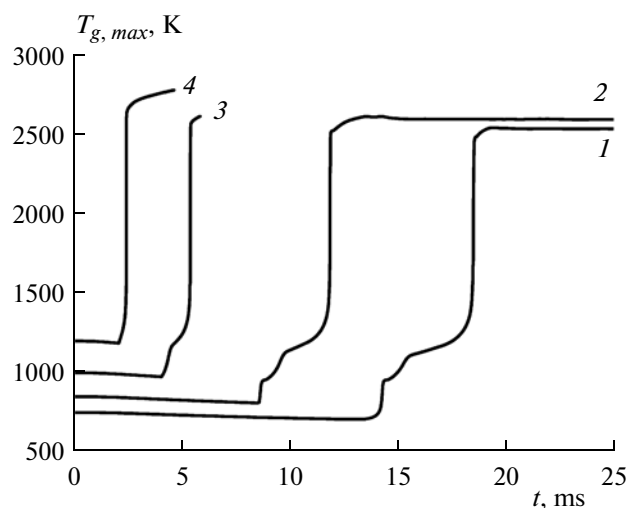
Fig. 11. Calculated time histories of the maximum temperature $T_{g, max}$ for the autoignition of stoichiometric n-tetradecane droplet–air mixtures at $d_0 = 60$ μm, $P_0 = 20$ atm, and $T_{g0} = 750$, 850, 1000, and 1200 K (curves 1–4).

diameter d^2 as functions of the time for the autoignition of droplet mixtures of the $C_{11}H_{24}$, $C_{13}H_{28}$, and $C_{16}H_{34}$ hydrocarbons at $d_0 = 60$ mm, $\Phi = 1$, $T_{g0} = 1000$ K, and $P_0 = 20$ atm. As can be seen from Fig. 12, the square of the droplet diameter first increases and then, as the $T_{g, max}(t)$ curve begins to ascend, starts to decrease in steps, and after a while, the $d^2(t)$ curve acquires an almost constant (negative) slope. The initial growth of droplet size can be explained by the thermal expansion of the liquid. This period is longer, the heavier the hydrocarbon and can exceed half of the droplet lifetime. The rate of descend of the curve $d^2(t)$

at its last, almost linear segment, characterizes the droplet burning rate constant k. In general, Fig. 12 suggests that the calculated autoignition delay time increases with n (from 11 to 16), whereas the burning rate constant k remains approximately unchanged. This result agrees qualitatively with the available experimental data.

Figure 13 quantitatively compares the calculated (curve) and measured (symbols [24, 25]) dependences of the ignition delay time for single n-decane droplets in air on the initial droplet diameter at $T_{g0} = 1220$ K and $P_0 = 1$ atm. The agreement between the experi-
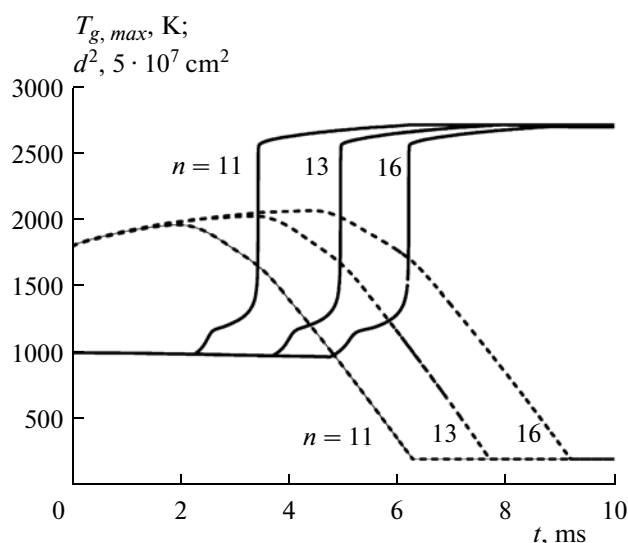

Fig. 12. Calculated time histories of the maximum temperature $T_{g, max}$ (solid curves) and the square of the droplet diameter d^2 (dashed) for the autoignition of hydrocarbon ($C_{11}H_{24}$, $C_{13}H_{28}$, $C_{16}H_{34}$) droplet–air mixtures at $d_0 = 60$ μm, $T_0 = 1000$ K, $P_0 = 20$ atm, and $\Phi = 1.0$.
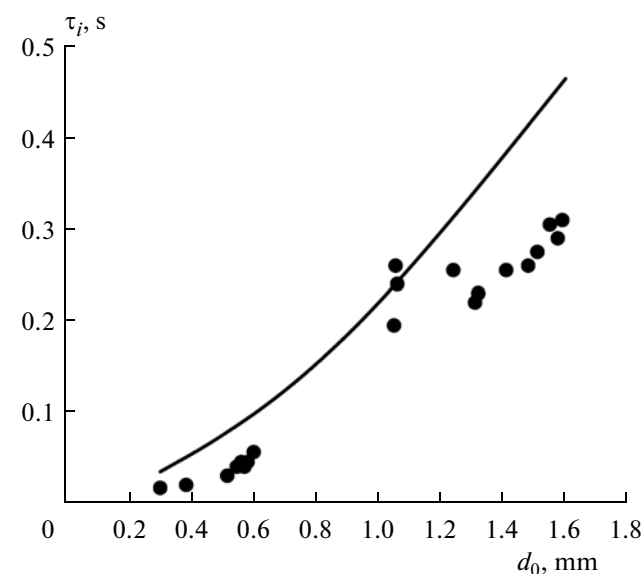

Fig. 13. Comparison of the calculated (curve) and measured (symbols [24, 25]) dependences of the ignition delay time τ_i on the initial diameter d_0 of n-hexadecane droplets at $T_{g0} = 1220$ K and $P_0 = 1$ atm.

mental data and the calculation results can be considered satisfactory, especially in view of the fact that, in contrast to the calculations, in the experiments, air flowed around the droplets at small Reynolds numbers.

CONCLUSIONS

In this work, a kinetic mechanism of the oxidation of paraffin hydrocarbons up to n-hexadecane ($C_{16}H_{34}$) was proposed. The mechanism includes the key processes that determine the reaction rate and the formation of the main intermediate and final products and has the status of a nonempirical detailed mechanism, since all the constant elementary reactions have a kinetic substantiation. The mechanism is based on the nonextensive approach to construction of reaction mechanisms, with emphasis not on the variety of products and reactions, but on the universality of the key pathways of the processes and of the main types of elementary steps. In passing from the detailed mechanism of the oxidation of the C_1-C_{10} hydrocarbons to that of the oxidation of n-hexadecane, the following simplifications were introduced: (1) schemes with the so-called double addition of oxygen (first to the peroxide radical, and then to its isomerized form) were not used—only the first addition was considered; (2) isoalkyl radicals and derivatives thereof were not considered as intermediates, since their oxidation is slower than the oxidation of the respective n-components. The resulting detailed kinetic mechanism of n-hexadecane oxidation turned out to be sufficiently compact, a feature important for constructing the oxidation mechanisms for more complex hydrocarbons.

The most important aspect of the mechanism is its stepwise nature, which manifests itself through the appearance of cool and blue flames at low autoignition temperatures. We calculated the characteristics of the autoignition and combustion of homogeneous mixtures of air with gaseous and liquid (droplets) hydrocarbons from n-undecane to n-hexadecane over a wide range of initial conditions and compared the calculation results with the experimental data, which turned out to be in satisfactory agreement. This suggests that the adopted principle of constructing the oxidation mechanisms for the hydrocarbons under study and the selected main reaction pathways are generally correct. The data file with the kinetic mechanism will be available at www.combex.ru.

ACKNOWLEDGMENTS

REFERENCES

1. C. Chevalier, P. Louessard, U. C. Muller, and J. Warnatz, in *Proceedings of the Joint Meeting of Soviet—Italian Sections of Combustion Institute* (Combust. Inst., Pisa, 1990), p. 5.
2. C. K. Westbrook, W. J. Pitz, O. Herbinet, et al., Combust. Flame **156**, 181 (2009).
3. A. B. Lebedev, A. N. Sekundov, A. M. Savel'ev, A. M. Starik, and N. S. Titova, in *Nonequilibrium physicochemical processes in gas flows and new principles of combustion organization,* Ed. by A. M. Starik (Torus Press, Moscow, 2011), p. 755 [in Russian].
4. N. S. Titova, S. A. Torokhov, and A. M. Starik, in *Nonequilibrium physicochemical processes in gas flows and new principles of combustion organization*, Ed. by A. M. Starik (Torus Press, Moscow, 2011), p. 88 [in Russian].
5. A. S. Sokolik, *Autoignition, combustion, flame and detonation in gases* (Akad. Nauk SSSR, Moscow, 1960) [in Russian].
6. B. Lewis and G. Elbe, *Combustion, flames and explosions of gases* (Academic Press, Orlando, 1987).
7. V. Ya. Basevich and S. M. Frolov, Russ. Chem. Rev. **76**, 867 (2007).
8. V. Ya. Basevich and S. M. Frolov, Khim. Fiz. **25** (11), 87 (2006).
9. V. Ya. Basevich, A. A. Belyaev, and S. M. Frolov, Russ. J. Phys. Chem. B **1**, 477 (2007).
10. V. Ya. Basevich, A. A. Belyaev, and S. M. Frolov, Russ. J. Phys. Chem. B **3**, 629 (2009).
11. V. Ya. Basevich, A. A. Belyaev, and S. M. Frolov, Russ. J. Phys. Chem. B **4**, 634 (2010).
12. V. Ya. Basevich, A. A. Belyaev, V. S. Posvyanskii, and S. M. Frolov, Russ. J. Phys. Chem. B **4**, 985 (2010).
13. V. Ya. Basevich, A. A. Belyaev, S. N. Medvedev, V. S. Posvyanskii, and S. M. Frolov, Russ. J. Phys. Chem. B **5**, 974 (2011).
14. R. C. Reid, J. M. Prausnitz, and T. K. Sherwood, *The properties of gases and liquids* (McGraw-Hill, New York, 1977).
15. S. S. Vasu, D. F. Davidson, and R. K. Hanson, in *Proceedings of the 26th international symposium on shock waves* (Gottingen, Germany, 2007), paper No. P2730.
16. D. F. Davidson, D. R. Haylett, and R. K. Hanson, Combust. Flame **155**, 108 (2008).
17. H.-P. S. Shen, J. Steinberg, J. Vanderer, et al., Energy Fuels **23**, 2482 (2009).
18. S. S. Vasu, D. F. Davidson, Z. Hong, et al., Proc. Combust. Inst. **32**, 173 (2009).
19. D. F. Davidson, Z. Hong, A. Pilla, et al., Proc. Combust. Inst. **33**, 151 (2011).
20. A. A. Belyaev and V. S. Posvyanskii, Algoritm. Program., Inform. Byull. Gos. Fond Algoritms Programs SSSR, No. 3, 35 (1985).
21. K. Kumar and C. J. Sung, Combust. Flame **151**, 209 (2007).
22. V. Ya. Basevich, A. A. Belyaev, S. N. Medvedev, V. S. Posvyanskii, F. S. Frolov, and S. M. Frolov, Russ. J. Phys. Chem. B **4**, 995 (2010).
23. A. S. Sokolik and V. Ya. Basevich, Zh. Fiz. Khim. **28**, 1935 (1954).
24. J.-J. Whang, C.-Y. Yukao, J.-T. Ho, and S.-C. Wong, Combust. Flame **110**, 366 (1997).
25. J.-R. Yang, C.-Y. Yukao, J.-J. Whang, and S.-C. Wong, Combust. Flame **123**, 266 (2000).